

1 **A bioinformatics tool for identifying intratumoral microbes from the ORIEN dataset**
2

3 Cankun Wang, MS¹; Anjun Ma, PhD^{1,2}; Megan E. McNutt, BS¹; Rebecca Hoyd, BS³; Caroline E.
4 Wheeler, BA³; Lary A. Robinson, MD⁴; Carlos H.F. Chan, MD, PhD⁵; Yousef Zakharia, MD⁶;
5 Rebecca D. Dodd, PhD⁷; Cornelia M. Ulrich, PhD, MS⁸; Sheetal Hardikar, PhD, MPH, MBBS⁸;
6 Michelle L. Churchman, PhD⁹; Ahmad A. Tarhini, MD, PhD¹⁰; Eric A. Singer, MD, MA, MS, FACS,
7 FASCO¹¹; Alexandra P. Ikeguchi, MD¹²; Martin D. McCarter, MD¹³; Nicholas Denko, MD, PhD¹⁴;
8 Gabriel Tinoco, MD, FACP³; Marium Husain, MD, MPH³; Ning Jin, MD³; Afaf E.G. Osman, MD¹⁵;
9 Islam Eljilany, PhD¹⁶; Aik Choon Tan, PhD¹⁷; Samuel S. Coleman, IV, MSBCB¹⁷; Louis Denko^{2,3};
10 Gregory Riedlinger, MD, PhD¹⁸; Bryan P. Schneider, MD¹⁹; Daniel Spakowicz, PhD^{2,3,\$}; and Qin
11 Ma, PhD^{1,2,\$}

12 ¹Department of Biomedical Informatics, College of Medicine, The Ohio State University, Columbus, OH, USA

13 ²Pelotonia Institute for Immuno-Oncology, The Ohio State University Comprehensive Cancer Center, Columbus, OH,
14 USA

15 ³Division of Medical Oncology, Department of Internal Medicine, The Ohio State University Comprehensive Cancer
16 Center, Columbus, OH, USA

17 ⁴Department of Thoracic Oncology, H. Lee Moffitt Cancer Center and Research Institute, Tampa, FL, USA

18 ⁵University of Iowa, Holden Comprehensive Cancer Center, Iowa City, IA, USA

19 ⁶Division of Oncology, Hematology and Blood & Marrow Transplantation, University of Iowa, Holden Comprehensive
20 Cancer Center, Iowa City, IA, USA

21 ⁷Department of Internal Medicine, University of Iowa, Iowa City, IA, USA

22 ⁸Department of Population Health Sciences, Huntsman Cancer Institute, University of Utah, Salt Lake City, UT, USA

23 ⁹Clinical & Life Sciences, M2GEN, Tampa, FL, USA

24 ¹⁰Departments of Cutaneous Oncology and Immunology, H. Lee Moffitt Cancer Center and Research Institute,
25 Tampa, FL, USA

26 ¹¹Department of Urologic Oncology, The Ohio State University Comprehensive Cancer Center, Columbus, OH, USA

27 ¹²Department of Hematology/Oncology, Stephenson Cancer Center of University of Oklahoma, Oklahoma City, OK,
28 USA

29 ¹³Department of Surgery, University of Colorado School of Medicine, Aurora, CO, USA

30 ¹⁴Department of Radiation Oncology, The Ohio State University Comprehensive Cancer Center, Columbus, OH, USA

31 ¹⁵Department of Internal Medicine, University of Utah, Salt Lake City, UT, USA

32 ¹⁶Clinical Science Lab -- Cutaneous Oncology, H. Lee Moffitt Cancer Center and Research Institute, Tampa, FL, USA

33 ¹⁷Departments of Oncological Science and Biomedical Informatics, Huntsman Cancer Institute, University of Utah,
34 Salt Lake City, UT, USA

35 ¹⁸Department of Precision Medicine, Rutgers Cancer Institute of New Jersey, New Brunswick, NJ, USA

36 ¹⁹Indiana University Simon Comprehensive Cancer Center, Indianapolis, IN, USA

37 ^{\$}Corresponding Author: Dr. Qin Ma. Email: qin.ma@osumc.edu

38 **RUNNING TITLE:** microbial graph attention (MEGA) for the tumor microbiome

39 **KEYWORDS:** deep learning, microbiome, cancer, tumor microbiome,

40 **SUBMISSION SECTION:** Precision Medicine & Biomarkers

41

42

43

44

45

46

47

48 **FINANCIAL SUPPORT**

49 This project was partly supported by The Ohio State University Comprehensive Cancer Center
50 and the National Institutes of Health (P30CA016058); The Huntsman Cancer Institute,
51 Comprehensive Cancer Center at the University of Utah (P30CA042014); The Ohio State
52 University Center for Clinical and Translational Science and the National Center for Advancing
53 Translational Sciences (8UL1TR000090-05); and the Oncology Research Information Exchange
54 Network (ORIEN) (21PRJNOVA009MCC).

55 **CONFLICTS OF INTEREST**

56 *Carlos Chan*: None related to this project. Other unrelated projects and clinical trials (Research
57 support from Checkmate Pharmaceuticals, Regeneron, Angiodynamics, Optimum Therapeutics)

58 *Yousef Zakharia*: Advisory Board: Bristol Myers Squibb, Amgen, Roche Diagnostics, Novartis,
59 Janssen, Eisai, Exelixis, Castle Bioscience, Genzyme Corporation, AstraZeneca, Array, Bayer,
60 Pfizer, Clovis, EMD serono, Myovant. Grant/research support from: Institution clinical trial support
61 from NewLink Genetics, Pfizer, Exelixis, Eisai. DSMC: Janssen Research and Development
62 Consultant honorarium: Pfizer, Novartis

63 *Ahmad Tarhini*: Contracted research grants with institution from Bristol Myers Squibb, Genentech-
64 Roche, Regeneron, Sanofi-Genzyme, Nektar, Clinigen, Merck, Acrotech, Pfizer, Checkmate,
65 OncoSec. Personal consultant/advisory board fees from Bristol Myers Squibb, Merck, Eisai, Instil
66 Bio Clinigin, Regeneron, Sanofi-Genzyme, Novartis, Partner Therapeutics, Genentech/Roche,
67 BioNTech, Concert AI, AstraZeneca outside the submitted work.

68 *Eric Singer*: Astellas/Medivation: research support (clinical trial); Johnson & Johnson: advisory
69 board; Merck: advisory board; Vyriad: advisory board; Aura Biosciences: data safety monitoring
70 board

71 *Gregory Riedlinger*: AstraZeneca advisory board

72 *Bryan Schneider*: Genentech-Research support (drug supply only); Pfizer-Research support
73 (Drug supply only); Foundation Medicine-research support (sequencing support)

74 **CODE AVAILABILITY**

75 The source code and tutorial of the MEGA package have been made available under the open-
76 source MIT license and can be freely accessed at <https://github.com/OSU-BMBL/MEGA>.

77 **AUTHOR CONTRIBUTIONS**

78 Resources: QM, AM, CW

79 Data curation: RH, CEW, DS, MC

80 Software: QM, AM, CW

81 Formal analysis: AM, CW

82 Supervision: QM

83 Validation: AM, CW

84 Investigation: AM, CW

85 Writing - original draft: QM, AM, CW

86 Writing - review and editing: all authors

87

88

89

90

91

92 **ABSTRACT**

93 Evidence supports significant interactions among microbes, immune cells, and tumor cells in at
94 least 10–20% of human cancers, emphasizing the importance of further investigating these
95 complex relationships. However, the implications and significance of tumor-related microbes
96 remain largely unknown. Studies have demonstrated the critical roles of host microbes in cancer
97 prevention and treatment responses. Understanding interactions between host microbes and
98 cancer can drive cancer diagnosis and microbial therapeutics (bugs as drugs). Computational
99 identification of cancer-specific microbes and their associations is still challenging due to the high
100 dimensionality and high sparsity of intratumoral microbiome data, which requires large datasets
101 containing sufficient event observations to identify relationships, and the interactions within
102 microbial communities, the heterogeneity in microbial composition, and other confounding effects
103 that can lead to spurious associations. To solve these issues, we present a bioinformatics tool,
104 MEGA, to identify the microbes most strongly associated with 12 cancer types. We demonstrate
105 its utility on a dataset from a consortium of 9 cancer centers in the Oncology Research Information
106 Exchange Network (ORIEN). This package has 3 unique features: species-sample relations are
107 represented in a heterogeneous graph and learned by a graph attention network; it incorporates
108 metabolic and phylogenetic information to reflect intricate relationships within microbial
109 communities; and it provides multiple functionalities for association interpretations and
110 visualizations. We analyzed 2704 tumor RNA-seq samples and MEGA interpreted the tissue-
111 resident microbial signatures of each of 12 cancer types. MEGA can effectively identify cancer-
112 associated microbial signatures and refine their interactions with tumors.

113

114 **SIGNIFICANCE**

115 Studying the tumor microbiome in high-throughput sequencing data is challenging because of the
116 extremely sparse data matrices, heterogeneity, and high likelihood of contamination. We present

117 a new deep-learning tool, microbial graph attention (MEGA), to refine the organisms that interact
118 with tumors.

119

120 INTRODUCTION

121 The study of microbial communities and their impact on human health has gained increasing
122 attention over the past decade (1). The role of intratumoral microbes in the tumor
123 microenvironment has become an increasingly important area in studying the development and
124 progression of cancer (2). The intratumoral microbiome affects outcomes in several cancers,
125 including *Fusobacterium nucleatum* in the development of colon cancer and *Helicobacter pylori*
126 in stomach cancer. To explore the relationship between the microbiome and cancer, large-scale
127 genomic datasets such as The Cancer Genome Atlas (TCGA) have been utilized. However,
128 limited attention has been given to the cancer-specific gene-microbe relationships. In this context,
129 the Oncology Research Information Exchange Network (ORIEN) provides a real-world dataset
130 consisting of clinical, genomic, and transcriptomic data collected under an institutional review
131 board (IRB)-approved common protocol known as Total Cancer Care. It represents a valuable
132 resource for identifying intratumoral microbes from various cancer types (3). Advances in
133 sequencing technologies have provided large-scale human tissue sequencing data, which
134 enables the characterization of the tissue-resident metagenome. However, exploring the links
135 between the intratumoral microbiome and cancer tissues is ongoing due to the difficulties in
136 obtaining clinical biopsies specifically dedicated to microbial profiling.

137

138 Here, we present Microbial Heterogeneous Graph Attention (MEGA), a deep learning-based
139 Python package for identifying cancer-associated intratumoral microbes. The model is trained on
140 ORIEN intratumoral microbial RNA sequencing (RNA-seq) data to identify microbial communities
141 associated with each of the 12 human cancer types. The core framework is a heterogeneous

142 graph transformer (HGT) (4) that can learn the importance and contribution of species to cancer
143 samples. We have shown the superior performance of HGT in characterizing cell-gene relations
144 from single-cell multi-omics datasets (5) and identifying sample-species relations (6) from The
145 Cancer Microbiome Atlas (TCMA) data (7). To demonstrate the effectiveness and credibility of
146 MEGA on the more complicated ORIEN data, we focus on 2 widely studied cancer types: colon
147 adenocarcinoma (COAD) and thyroid carcinoma (THCA). By leveraging metabolic and
148 phylogenetic relationships, MEGA was able to capture the association of low attention score
149 microbes, suggesting the importance of integrating multiple types of data in identifying cancer-
150 associated microbes. We believe that MEGA offers a comprehensive and nuanced approach to
151 identifying cancer-associated intratumoral microbes in the ORIEN dataset, which could ultimately
152 serve as potential targets for further study and therapy development.

153

154 **METHODS**

155 **Study Design**

156 Established in 2014, the Oncology Research Information Exchange Network (ORIEN) is an
157 alliance of 18 US cancer centers. All ORIEN alliance members utilize a standard IRB-approved
158 protocol: Total Cancer Care® (TCC). As part of the TCC, participants agree to have their clinical
159 data followed over time, to undergo germline and tumor sequencing, and to be contacted in the
160 future by their provider if an appropriate clinical trial or other study becomes available (8). TCC is
161 a prospective cohort study where a subset of patients elect to be enrolled in the ORIEN Avatar
162 program, which provides research use only (RUO)-grade whole-exome tumor sequencing, RNA-
163 seq, germline sequencing, and collection of deep longitudinal clinical data with lifetime follow-up.
164 Nationally, over 325,000 participants have enrolled in TCC. M2GEN, the commercial and
165 operational partner of ORIEN, harmonizes all abstracted clinical data elements and molecular
166 sequencing files into a standardized, structured format to enable the aggregation of de-identified
167 data for sharing across the network. Data access was approved by the IRB in an Honest Broker

168 protocol (2015H0185) and Total Cancer Care protocol (2013H0199) in coordination with M2GEN
169 and participating ORIEN members.

170

171 **Sequencing Methods**

172 ORIEN Avatar specimens undergo nucleic acid extraction and sequencing at HudsonAlpha
173 (Huntsville, AL) or Fulgent Genetics (Temple City, CA). For frozen and OCT tissue DNA extraction,
174 Qiagen QIASymphony DNA purification is performed, generating a 213 bp average insert size.
175 For frozen and OCT tissue RNA extraction, Qiagen RNAeasy plus mini kit is performed,
176 generating 216 bp average insert size. For formalin-fixed paraffin-embedded (FFPE) tissue, a
177 Covaris Ultrasonication FFPE DNA/RNA kit is utilized to extract DNA and RNA, generating a 165
178 bp average insert size. RNA-seq is performed using the Illumina TruSeq RNA Exome with single
179 library hybridization, cDNA synthesis, library preparation, and sequencing (100 bp paired reads
180 at Hudson Alpha, 150 bp paired reads at Fulgent) to a coverage of 100M total reads/50M paired
181 reads.

182

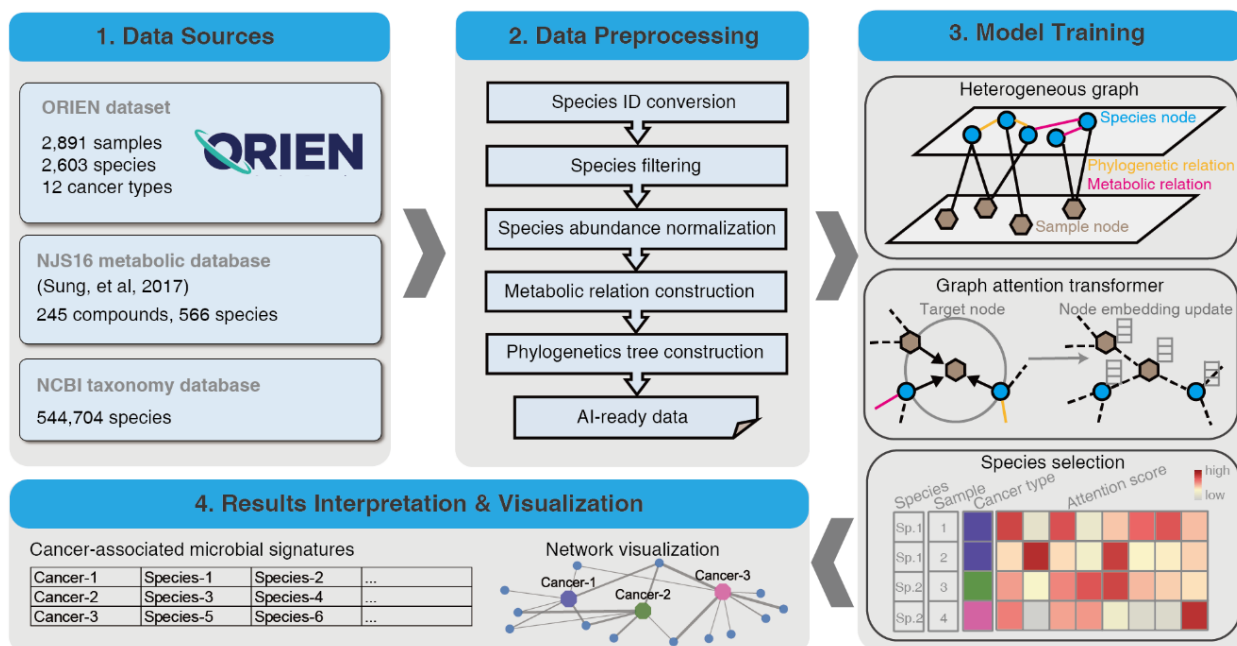
183 **Microbe Abundance and Diversity**

184 RNA-seq reads are used to calculate microbe abundances using the {exotic} pipeline, as
185 described previously (3). Briefly, reads are aligned first to the human reference genome, and then
186 unaligned reads are mapped to a database of bacteria, fungi, archaea, viruses, and eukaryotic
187 parasites. The observed microbes then proceed through a series of filtering steps to carefully and
188 conservatively remove contaminants before batch correction and normalization. Diversity
189 measures were estimated by calculating the Shannon and Simpson indices, as well as Chao1,
190 ACE, and inverse Simpson using the R package vegan.

191

192 The input dataset for MEGA includes the microbiome matrix and the sample metadata of the
193 cancer types. The raw counts of the ORIEN microbiome matrix consist of 2603 species in 2891

194 samples. The sample metadata is a two-column matrix that describes the label of the total of 12
195 cancer types at each sample. The NJS16 metabolic database (9) is a literature-curated
196 interspecies network of the human gut microbiota, composed of approximately 570 microbial
197 species and 3 human cell types metabolically interacting through more than 4400 small-molecule
198 transport and macromolecule degradation events. We utilized the R package *taxizedb* to access
199 the National Center for Biotechnology Information (NCBI) taxonomy database (10). It was
200 integrated to prepare for the taxonomy ID to taxonomy name conversion and to extract additional
201 phylogenetic relationships from the ORIEN data (see **Figure 1 – Data Sources**).
202



203
204 **Figure 1. Overview of the MEGA workflow.** Four main steps were included in carrying out model training and
205 biological gene network inference. MEGA uses ORIEN datasets and two database dependencies as the data sources.
206 Preprocessing steps are employed to generate artificial intelligence (AI)-ready data for graph neural network training.
207 After deep learning model training, the cancer-associated microbial signatures were selected based on the attention
208 scores of each species at the sample level. The final results of the identified cancer-associated microbial communities
209 have been provided in a tabular format and are available for additional visualization.
210

211 Data Preprocessing

212 We initially converted the organism's name to a standard taxonomy ID using the *taxizedb* package.
213 Species were filtered by removing those that expressed less than 0.1% of the total species. After

214 filtering, 2,266 species were obtained. To normalize the microbiome matrix, we scaled the values
215 in each sample of the matrix that summed to 1. This method ensures that the contribution of each
216 feature to the total sum is proportional to its relative abundance in the sample. We used the
217 normalized matrix as the basis for downstream analyses. Specifically, we generated the metabolic
218 relationship network by comparing the total species list in the ORIEN matrix with the NJS16
219 metabolic database. In this network, an edge was placed between two species if they shared the
220 same metabolic compound shown in the NJS16 database. Similarly, for the phylogenetic relation
221 network, we compared the total species list in the ORIEN matrix with the NCBI taxonomy
222 database, placing an edge that links two species if they share the same genus information. The
223 processed data, including the normalized abundance matrix, metabolic relationship network, and
224 phylogenetic relation network, served as artificial intelligence (AI)-ready data for model training
225 (**see Figure 1 – Data Processing**).

226

227 **Model Training**

228 The main MEGA model was implemented in PyTorch (11) (v1.4.0) and was trained on an NVIDIA
229 A100 graphics processing unit (GPU) for 50 epochs (approximately 15 minutes). We utilized our
230 previously developed heterogeneous graph transformer model for model training (6). The input
231 graph incorporates both species and sample nodes, along with the relations among them as
232 edges. By capturing both neighbor and global topological features among samples and species,
233 the model was able to construct sample-sample and species-species relations simultaneously.
234 We used two autoencoders to generate the initial embeddings for the heterogeneous graph. This
235 allowed the representation of each node as a dense vector, which can be used as input for the
236 deep learning model. Meanwhile, we were able to reduce the dimensionality of each species and
237 sample, resulting in an initial embedding size of 256 dimensions for all nodes in the graph. The
238 complete heterogeneous graph embedding was subsequently passed to a graph attention
239 transformer, which was trained to learn the relations between sample and species. MEGA adopts

240 a heterogeneous multi-head attention mechanism to model the overall topological information
241 (global relationships) and neighbor message passing (local relationships) on the heterogeneous
242 graph. We used the Adam optimizer with a learning rate of 0.003 and default settings for other
243 hyperparameters: n_hid=128, KL_COEF=0.00005, and THRES=3. The Focal Loss function was
244 used to quantify the differences between the predicted cancer type labels and true cancer type
245 labels. The learning rate was reduced by a factor of 0.5 when the evaluation metric stopped
246 improving for 5 epochs. The heterogeneous graph representation learning facilitated the
247 embedding of samples and species simultaneously using the transformer, yielding the attention
248 score as an important training outcome. This score represents the importance of a source node
249 to a target node. We extracted the attention scores from source nodes spanning from species to
250 sample. A high attention score between a given species and a sample indicates that the species
251 was highly represented in the sample. We leveraged this information to identify microbial
252 signatures associated with specific cancer types. We accomplished this by counting the number
253 of samples within the cancer type for each species with high attention scores. Species with a *p*-
254 value less than 0.05 were considered to be significantly associated with the cancer type. These
255 reliable microbial signatures were selected and served as the final output of MEGA (**see Figure**
256 **1 – Model Training**).

257

258 **Results Interpretation and Visualization**

259 The final output of MEGA is a tab-delimited list, where each row represents each cancer type
260 followed by identified microbial signatures. The results can be visualized in UpSet plots (12) and
261 Cytoscape networks (13). UpSet plots are a powerful visualization technique designed to display
262 complex set data with more than 3 intersecting sets. This method provides an intuitive and
263 comprehensive means of exploring the relationships between sets and their overlaps, allowing
264 for a more nuanced interpretation of the underlying data. Cytoscape is a widely used open-source
265 software platform that offers a suite of tools for the visualization, analysis, and modeling of

266 complex networks. To leverage the strengths of Cytoscape's capabilities, the RCy3 R package
267 (14) was utilized to implement the network visualization aspect of MEGA. Through the use of
268 RCy3's REST application programming interface (API), users can seamlessly access the full
269 feature set of Cytoscape within the R programming environment. Users can import network works
270 directly to Cytoscape with the predefined layout and theme using MEGA output files. The network
271 comprises cancer-species nodes, with the thickness of the edges reflecting the attention weight
272 scores. In addition, phylogenetic or metabolic relationships between species are represented by
273 additional edges. This approach allows for a comprehensive and nuanced exploration of the
274 relationships between cancer and species, providing valuable insights into the underlying
275 biological processes and pathways involved. The attention weight scores, represented by the
276 edge thickness, highlight the key connections and interactions within the network, enabling
277 researchers to effectively identify potential targets for further study (**see Figure 1 – Results**
278 **Interpretation & Visualization**). Additional tutorials on generating both UpSet plots and
279 Cytoscape networks can be found in the MEGA GitHub repository [https://github.com/OSU-](https://github.com/OSU-BMBL/MEGA)
280 BMBL/MEGA.

281

282 **Implementation**

283 MEGA was developed using Python 3.7.12 with PyTorch v1.4.0 and torch-geometric v1.4.3. The
284 MEGA GPU mode was tested in CUDA v11.6 on a Red Hat Enterprise 7 Linux system 8.3, which
285 featured 128-core AMD Epic central processing units (CPUs), NVIDIA A100-PCIE-80GB GPUs,
286 and 1TB RAM. Similarly, the MEGA CPU mode was tested on the Ohio Supercomputer Center
287 Pitzer cluster, which incorporated Intel Xeon Gold 6148 CPUs and 64GB RAM. MEGA was
288 versioned and uploaded to the Python Package Index (PyPI) using Python-Versioneer, a tool that
289 simplifies the management of version numbers in a software project. By subjecting the software
290 to extensive testing in both GPU and CPU modes, we were able to ensure that MEGA functions

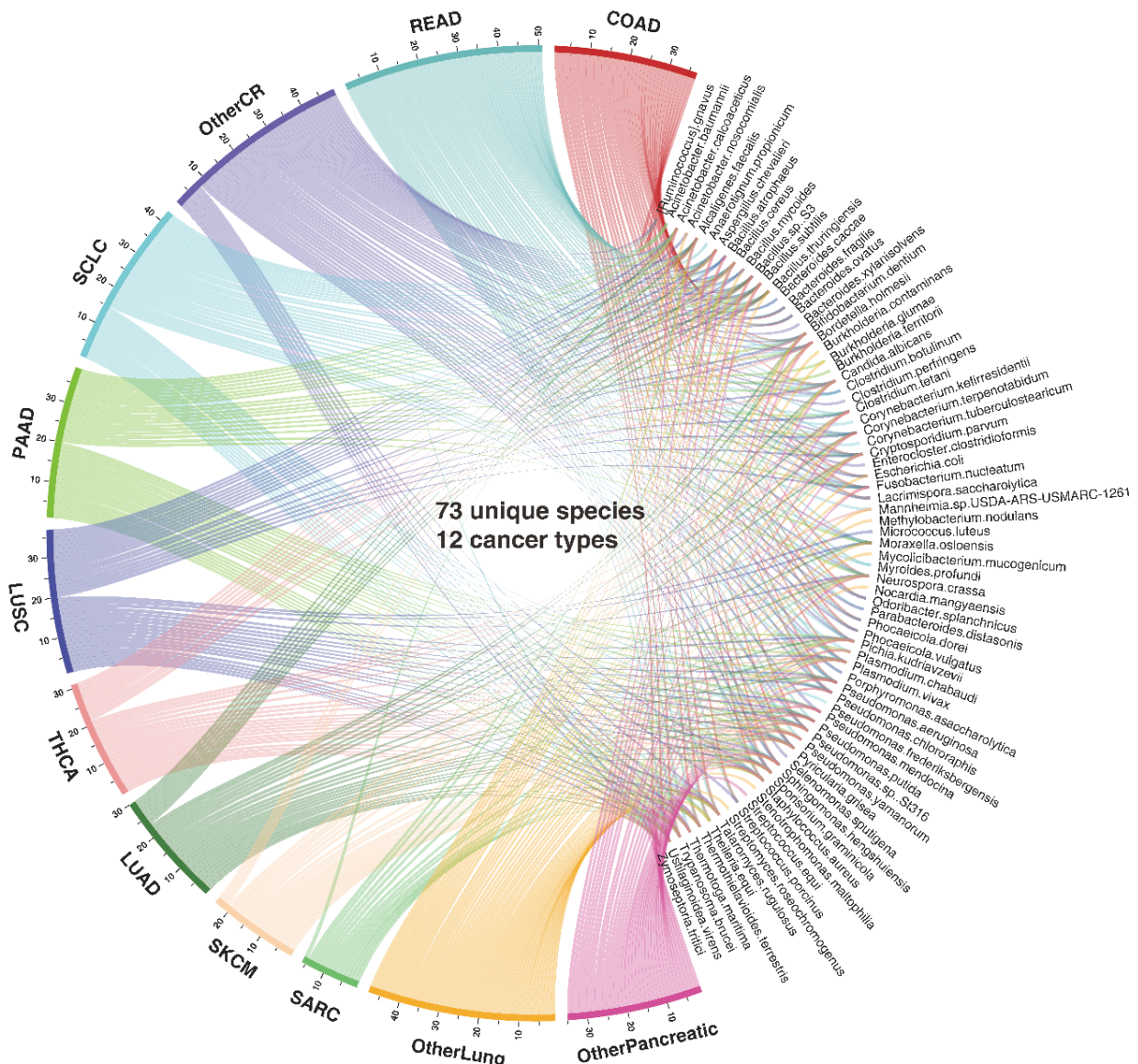
291 effectively and efficiently across a range of computational architectures, ultimately providing users
292 with a reliable and versatile tool.

293

294 **RESULTS**

295 **MEGA Identifies Intratumoral Microbes from 12 Cancer Types in the ORIEN Dataset**

296 Overall, MEGA is a deep learning package for identifying cancer-associated intratumoral
297 microbes. It consists of 4 main steps: (1) Collect the ORIEN dataset, Human NJS16 metabolic
298 database [2], and NCBI taxonomy database; (2) Preprocess ORIEN dataset as input for the deep
299 learning model; (3) Train the graph attention transformer using a heterogeneous graph; and (4)
300 Interpret cancer-associated intratumoral microbes. MEGA identified microbial communities that
301 consist of 73 unique species from 12 cancer types in the ORIEN data (**see Figure 2 and**
302 **Supplementary Table S1**). Our analysis revealed that 15 species were shared across all 12
303 cancer types. Notably, 8 species were uniquely shared among COAD, rectum adenocarcinoma
304 (READ), and other colorectal cancer (OtherCR). This group of 8 species represented the second-
305 highest number of shared species across all intersections, and their shared presence is consistent
306 with the fact that these cancers all originate in the large intestine, as in the case of colorectal
307 cancer (CRC) (**see Supplementary Figure S1**).



308

309 **Figure 2. Circos plot representation of the distribution of identified species and cancer types.** The segment
310 length for each cancer type is proportional to the ratio of the total number of detected species within that cancer type,
311 and individual ribbons are linked to their respective species. The cancer types are abbreviated as COAD (Colon
312 Adenocarcinoma); LUAD (Lung Adenocarcinoma); LUSC (Lung Squamous Cell Carcinoma); OtherCR (Other colorectal
313 cancer types not specified); OtherLung (Other lung cancer types not specified); OtherPancreatic (Other pancreatic
314 cancer types not specified); PAAD (Pancreatic Adenocarcinoma); READ (Rectum Adenocarcinoma); SARC (Sarcoma);
315 SCLC (Small Cell Lung Cancer); SKCM (Skin Cutaneous Melanoma); and THCA (Thyroid Carcinoma).

316

317 **MEGA Identifies Cancer-associated Microbes in Colon Adenocarcinoma and Thyroid**

318

Carcinoma

319

To demonstrate the data analysis and interpretation capabilities of MEGA, we focused on case
320 studies in COAD and THCA. These cancers were chosen for their contrasting levels of attention

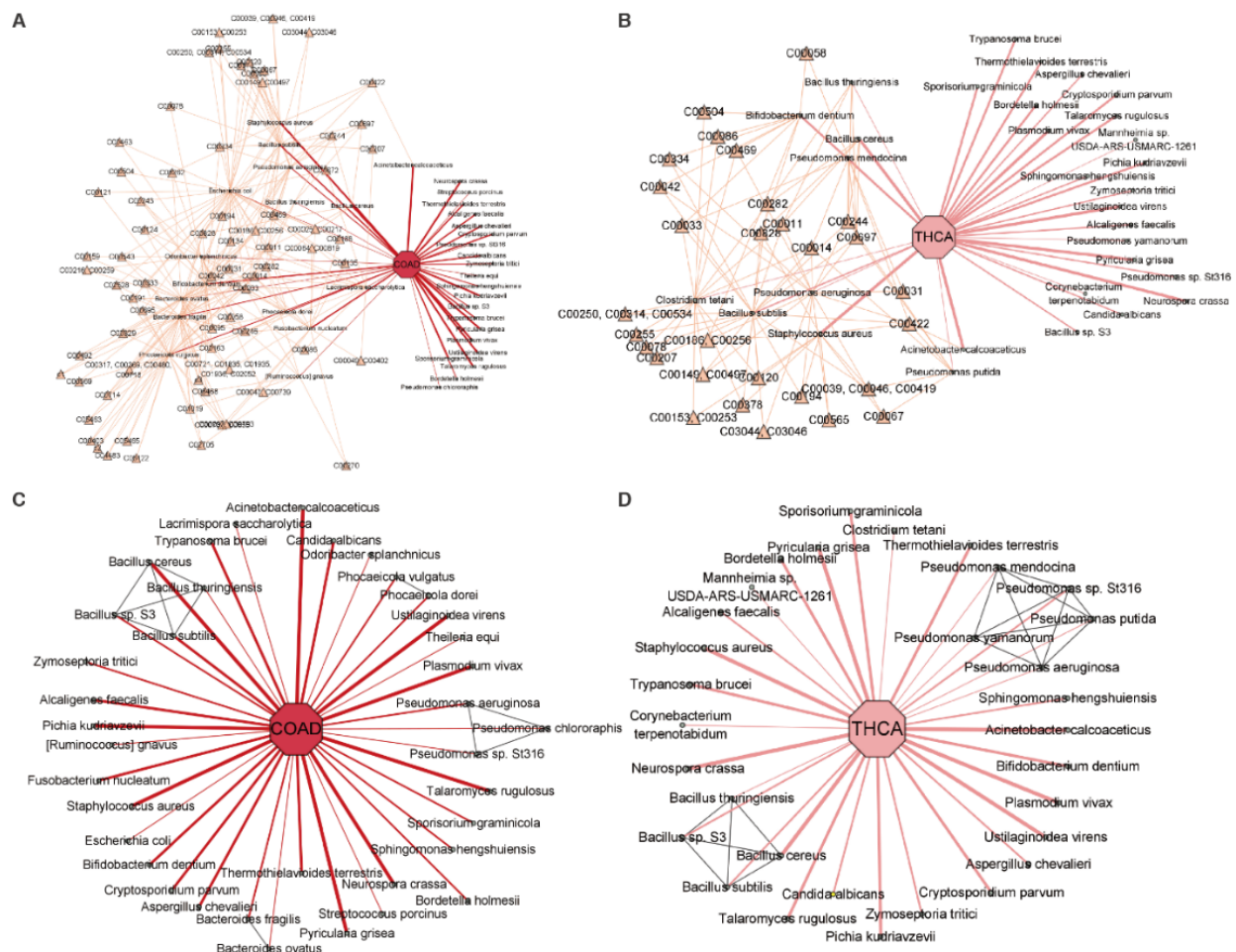
321 within the tumor microbiome research community. COAD has been relatively well studied in
322 relation to its associations with tumor microbes, whereas THCA has not yet received significant
323 attention. By using these well-known cases as a benchmark, we validated the effectiveness and
324 credibility of MEGA. COAD is a common malignant tumor in the digestive tract (15). Increased
325 evidence suggests that intestinal microbiota was crucial in developing CRC (16). Our analysis
326 revealed that 8 microbial species were uniquely shared among the CRC types COAD, READ, and
327 OtherCR. These species are *Bacteroides fragilis*, *Ruminococcus gnavus*, *Bacteroides ovatus*,
328 *Lacrimispora saccharolytica*, *Odoribacter splanchnicus*, *Phocaeicola dorei*, *Phocaeicola vulgatus*,
329 and *Streptococcus porcinus*. Notably, 3 of these species—*Bacteroides fragilis*, *Ruminococcus*
330 *gnavus*, and *Bacteroides ovatus*—were found to be consistent with previously validated
331 experimental results (17-22). MEGA successfully identified these species by integrating metabolic
332 and phylogenetic relationships in the model training process.

333

334 By integrating metabolic relationships, MEGA was able to capture the association even when a
335 relatively low attention score is presented. For instance, *Fusobacterium nucleatum* shows high
336 attention scores among the identified species in COAD, and its infection promotes CRC
337 progression by changing the mucosal microbiota and colon transcriptome in a mouse model (17).
338 *Ruminococcus gnavus* has a low attention score and the abundance was shown to have a
339 significant negative correlation with CRC tumor numbers and disease score (18). *Fusobacterium*
340 *nucleatum* and *Ruminococcus gnavus* shared the same compound C00270: N-
341 Acetylneuraminate acid, where the intercellular adhesive events may play an important role in
342 tumor angiogenesis, metastasis, and growth control in COAD (19). *Ruminococcus gnavus* also
343 shared the same compound C01019: L-Fucose with *Bacteroides fragilis*. Recent studies found
344 that *Bacteroides fragilis* toxin can contribute to COAD formation (20), while fucose-bound
345 liposomes carrying anticancer drugs could serve as a new strategy for the treatment of CRC
346 patients (21) (**see Figure 3A**). THCA has increased substantially in many countries during the

347 past few decades (23). The species related to compound C00422: Triacylglycerol, including
348 *Pseudomonas aeruginosa* and *Staphylococcus aureus* were found in THCA groups. Recent
349 studies suggest that elevated triglyceride levels may be a potential biomarker for identifying
350 individuals at a higher risk of developing thyroid cancer (24) (see Figure 3B). The full metabolic
351 relationships for all 12 cancer types can be found in **Supplementary Table S2**.

352



353

354 **Figure 3. Network visualization of identified microbial communities in COAD and THCA.** The cancer-type nodes
355 were highlighted by an octagon shape, while the microbial species nodes were highlighted in a circle shape. The
356 thickness of the edges in the network reflects the attention weight scores, indicating the strength of the relationship
357 between the species and cancer. In addition, the metabolic compound nodes were highlighted with a yellow triangle
358 shape, while the phylogenetic relationship edges were highlighted in gray. (A) COAD-associated microbes highlighted
359 with metabolic compound. (B) THCA-associated microbes highlighted with metabolic compound. (C) COAD-associated
360 microbes highlighted with phylogenetic relationships. (D) THCA-associated microbes highlighted with phylogenetic
361 relationships.

362

363 By integrating phylogenetic relationships, MEGA was able to capture associations with relatively
364 low attention scores. A previous study found that *Bacteroides ovatus* may be one of the dominant
365 species in colon cancer (22). Although *Bacteroides ovatus* had a relatively low attention score,
366 MEGA can identify it using the phylogenetic association with *Bacteroides fragilis*, which has a
367 high attention score (see Figure 3C). We found that *Pseudomonas mendocina*, *Pseudomonas*
368 *putida*, and *Pseudomonas yamanorum* were uniquely identified in the *Pseudomonas* genus in
369 THCA, in contrast to COAD. This aligns with the study showing the predominance of
370 *Pseudomonas* in THCA (see Figure 3D) (25). The phylogenetic relationships for all 12 cancer
371 types can be found in **Supplementary Table S3**.

372

373 **DISCUSSION**

374 The development of MEGA represents a significant step forward in identifying and interpreting
375 cancer-associated intratumoral microbes. The deep learning package presented in this study
376 utilizes RNA-seq data from the ORIEN dataset to identify microbial signatures associated with 12
377 different cancer types. By leveraging the power of graph attention transformers, MEGA can
378 capture both local and global topological features of the heterogeneous graph, resulting in a more
379 comprehensive and nuanced understanding of the underlying biological processes and pathways
380 involved. The application of MEGA to the ORIEN dataset has provided valuable insights into the
381 role of intratumoral microbes in cancer. The analysis revealed 73 unique species associated with
382 the 12 cancer types studied. Notably, 15 species were shared across all 12 cancer types,
383 highlighting the potential importance of these microbes in cancer development and progression.

384

385 As a next step, we will further compare the cancer-associated intratumoral microbes identified
386 from TCMA and ORIEN data using MEGA to provide a more comprehensive understanding of
387 the role of intratumoral microbes in relation to cancer biology and host immunology. In the long
388 run, the genotype-tissue expression (GTEx) data can be involved as control samples to identify

389 relationships specific to tumors. In addition, applying MEGA to single-cell RNA-seq data could
390 provide a more detailed understanding of the interactions between microbial communities and
391 tumor cells at the cellular level. It may give us a new angle to characterize tumor heterogeneity
392 based on intratumoral microbiome diversities. In conclusion, the development of MEGA
393 represents an important advance in identifying cancer-associated intratumoral microbes. Our
394 analysis of ORIEN data using MEGA revealed the presence of unique microbial signatures in
395 specific cancer types, which may provide new targets for therapeutic intervention.

396
397

SUPPLEMENTARY DATA

398 Supplementary Table S1. Identified microbial signatures with normalized attention weights.

399 Supplementary Table S2. Metabolic compounds relationships microbial signatures.

400 Supplementary Table S3. Phylogenetic relationships of microbial signatures.

401
402

ACKNOWLEDGMENTS

403 This work was supported by the Pelotonia Institute of Immuno-Oncology (PIIO). The content is
404 solely the responsibility of the authors and does not necessarily represent the official views of the
405 PIIO. The authors acknowledge the support and resources of the Ohio Supercomputer Center
406 (PAS1695, PCON0005). We would like to thank Angela Dahlberg, Editor, Division of Medical
407 Oncology at The Ohio State University Comprehensive Cancer Center, for editing and
408 proofreading the manuscript.

409
410

REFERENCES

- 412 1. Cho, I. and Blaser, M.J. (2012) The human microbiome: at the interface of health and
413 disease. *Nat Rev Genet*, **13**, 260-270.
- 414 2. Chen, Y., Wu, F.H., Wu, P.Q., Xing, H.Y. and Ma, T. (2022) The Role of The Tumor
415 Microbiome in Tumor Development and Its Treatment. *Front Immunol*, **13**, 935846.
- 416 3. Hoyd, R., Wheeler, C.E., Liu, Y., Singh, M.J., Muniak, M., Denko, N., Carbone, D., Mo, X.
417 and Spakowicz, D. (2022) Exogenous sequences in tumors and immune cells (exotic): a
418 tool for estimating the microbe abundances in tumor RNAseq data.
- 419 4. Hu, Z., Dong, Y., Wang, K. and Sun, Y. (2020) Heterogeneous Graph Transformer.
- 420 5. Ma, A., Wang, X., Li, J., Wang, C., Xiao, T., Liu, Y., Cheng, H., Wang, J., Li, Y., Chang, Y.
421 et al. (2023) Single-cell biological network inference using a heterogeneous graph
422 transformer. *Nat Commun*, **14**, 964.
- 423 6. Liu, Z., Sun, Y., Ma, A., Wang, X., Xu, D., Spakowicz, D., Ma, Q. and Liu, B. (2023) An
424 explainable graph neural framework to identify cancer-associated intratumoral microbial
425 communities. *bioRxiv*, 2023.2004.2016.537088.
- 426 7. Dohlman, A.B., Arguijo Mendoza, D., Ding, S., Gao, M., Dressman, H., Iliev, I.D., Lipkin,
427 S.M. and Shen, X. (2021) The cancer microbiome atlas: a pan-cancer comparative

428 analysis to distinguish tissue-resident microbiota from contaminants. *Cell Host Microbe*,
429 **29**, 281-298 e285.

430 8. Dalton, W.S., Sullivan, D., Ecsedy, J. and Caligiuri, M.A. (2018) Patient Enrichment for
431 Precision-Based Cancer Clinical Trials: Using Prospective Cohort Surveillance as an
432 Approach to Improve Clinical Trials. *Clin Pharmacol Ther*, **104**, 23-26.

433 9. Sung, J., Kim, S., Cabatbat, J.J.T., Jang, S., Jin, Y.-S., Jung, G.Y., Chia, N. and Kim, P.-
434 J. (2017) Global metabolic interaction network of the human gut microbiota for context-
435 specific community-scale analysis. *Nature Communications*, **8**, 15393.

436 10. Schoch, C.L., Ciufo, S., Domrachev, M., Hotton, C.L., Kannan, S., Khovanskaya, R., Leipe,
437 D., Mcveigh, R., O'Neill, K., Robbertse, B. *et al.* (2020) NCBI Taxonomy: a comprehensive
438 update on curation, resources and tools. *Database*, **2020**, baaa062.

439 11. Paszke, A., Gross, S., Massa, F., Lerer, A., Bradbury, J., Chanan, G., Killeen, T., Lin, Z.,
440 Gimelshein, N., Antiga, L. *et al.* (2019) PyTorch: An Imperative Style, High-Performance
441 Deep Learning Library.

442 12. Lex, A., Gehlenborg, N., Strobelt, H., Vuillemot, R. and Pfister, H. (2014) UpSet:
443 Visualization of Intersecting Sets. *IEEE transactions on visualization and computer
444 graphics*, **20**, 1983-1992.

445 13. Shannon, P., Markiel, A., Ozier, O., Baliga, N.S., Wang, J.T., Ramage, D., Amin, N.,
446 Schwikowski, B. and Ideker, T. (2003) Cytoscape: A Software Environment for Integrated
447 Models of Biomolecular Interaction Networks. *Genome Research*, **13**, 2498-2504.

448 14. Gustavsen, J.A., Pai, S., Isserlin, R., Demchak, B. and Pico, A.R. (2019). F1000Research.

449 15. Xie, Y.-H., Chen, Y.-X. and Fang, J.-Y. (2020) Comprehensive review of targeted therapy
450 for colorectal cancer. *Signal Transduction and Targeted Therapy*, **5**, 1-30.

451 16. Lucas, C., Barnich, N. and Nguyen, H.T.T. (2017) Microbiota, Inflammation and Colorectal
452 Cancer. *International Journal of Molecular Sciences*, **18**, 1310.

453 17. Wu, N., Feng, Y.-Q., Lyu, N., Wang, D., Yu, W.-D. and Hu, Y.-F. (2022) Fusobacterium
454 nucleatum promotes colon cancer progression by changing the mucosal microbiota and
455 colon transcriptome in a mouse model. *World Journal of Gastroenterology*, **28**, 1981-1995.

456 18. Alrafas, H.R., Busbee, P.B., Chitrala, K.N., Nagarkatti, M. and Nagarkatti, P. (2020)
457 Alterations in the Gut Microbiome and Suppression of Histone Deacetylases by
458 Resveratrol Are Associated with Attenuation of Colonic Inflammation and Protection
459 Against Colorectal Cancer. *Journal of Clinical Medicine*, **9**, 1796.

460 19. Dimitroff, C.J., Pera, P., Dall'Olio, F., Matta, K.L., Chandrasekaran, E.V., Lau, J.T. and
461 Bernacki, R.J. (1999) Cell surface n-acetylneuraminc acid alpha2,3-galactoside-
462 dependent intercellular adhesion of human colon cancer cells. *Biochemical and
463 Biophysical Research Communications*, **256**, 631-636.

464 20. Cheng, W.T., Kantilal, H.K. and Davamani, F. (2020) The Mechanism of Bacteroides
465 fragilis Toxin Contributes to Colon Cancer Formation. *The Malaysian Journal of Medical
466 Sciences : MJMS*, **27**, 9-21.

467 21. Osuga, T., Takimoto, R., Ono, M., Hirakawa, M., Yoshida, M., Okagawa, Y., Uemura, N.,
468 Arihara, Y., Sato, Y., Tamura, F. *et al.* (2016) Relationship Between Increased

469 Fucosylation and Metastatic Potential in Colorectal Cancer. *JNCI: Journal of the National*
470 *Cancer Institute*, **108**, djw210.

471 22. He, T., Cheng, X. and Xing, C. (2021) The gut microbial diversity of colon cancer patients
472 and the clinical significance. *Bioengineered*, **12**, 7046-7060.

473 23. Kitahara, C.M. and Sosa, J.A. (2016) The changing incidence of thyroid cancer. *Nature*
474 *Reviews Endocrinology*, **12**, 646-653.

475 24. Alkurt, E.G., Şahin, F., Tutan, B., Canal, K. and Turhan, V.B. (2022) The relationship
476 between papillary thyroid cancer and triglyceride/glucose index, which is an indicator of
477 insulin resistance. *European Review for Medical and Pharmacological Sciences*, **26**,
478 6114-6120.

479 25. Yuan, L., Yang, P., Wei, G., Hu, X.e., Chen, S., Lu, J., Yang, L., He, X. and Bao, G. (2022)
480 Tumor microbiome diversity influences papillary thyroid cancer invasion. *Communications*
481 *Biology*, **5**, 1-9.

482